Available online at www.sciencedirect.com

ScienceDirect

Procedia CIRP 31 (2015) 387 – 392

www.elsevier.com/locate/procedia

15th CIRP Conference on Modelling of Machining Operations

Analysis of Process Forces for the Precision Honing of Small Bores

Uwe Moos[a,*], Dirk Bähre[a]

[a]*Institute of Production Engineering, Saarland University, D-66123 Saarbrücken, Germany*

[*] Corresponding author. Tel.: +49-681-302-57559; Fax: +49-681-302-4858. *E-mail address:* u.moos@mx.uni-saarland.de

Abstract

For the honing process the chip removal and therewith the material removal rate and the surface of the part after honing depend on the cutting pressure between the honing stone and the workpiece. In this paper an analytical model of the honing tool is used to make the contact surface between honing stone and workpiece as well as the in-process forces at the honing stone accessible from the geometry, positions and given process loads at the honing unit over different approaches without additional sensors. Exemplary paths of the cutting pressure dependent on the stroke position are then given for an assumed constant axial feeding force on the cone including friction as well as for an assumed constant torque along the axis of the honing tool. It is found that for active movement of the feeding cone the calculations from the feeding force and the torque along the tool are approximately equal. For reactive feeding movement because of high normal forces at the honing stone self-locking can occur for the given tool with small cone angle because of friction at the cone.

Peer-review under responsibility of the International Scientific Committee of the "15th Conference on Modelling of Machining Operations

Keywords: Honing; Modelling; Process Control

1. Introduction

Honing is a manufacturing process that is mainly used for workpieces with high requirements on production accuracy. Especially for the machining of cylindrical bores, honing can keep small tolerances with high process reliability for features as e.g. bore diameter, roundness, cylinder shape, surface roughness and ratio between the bearing contact area and the total area. This causes very low running-in wear at guiding surfaces, e.g. for piston raceways.

Honing is an abrasive process with geometrically undefined cutting edges. Similar processes with undefined cutting edges, but different kinematics are e.g. grinding and lapping. In contrast to grinding, the cutting grains in the honing process mostly are in continuous contact with the surface of the workpiece.

The path of the grains is induced by the special kinematics of honing. Especially the feeding velocity is a decisive factor for the honing process because the difference between feeding velocity and material removal rate assigns the normal force to the honing stone. This normal force determines the cutting ability of the stone and thus influences the material removal rate again. [1] confirms that next to the cutting velocity the cutting pressure has the strongest impact on the material removal rate of honing.

In the industrial application there are two prevalent systems to induce the feeding movement: force-closure systems define the feeding force on the tool, e.g. by a defined pressure in a hydraulic cylinder. In contrast, form-closure systems define the movement of the feeding cone in the tool, e.g. by a mechanical screw gear. Especially for the precision honing of bores with diameters beyond approximately 50 mm, form-closure feeding systems are mainly used because of possibly higher stock removal rates and higher switch-off accuracy for the diameter of the honed bore.

To further enhance the process capability several closed-loop controls for the feeding movement have been developed in the past instead of the known open-loop control [2, S. 336 ff]. A decisive factor for those controls is the estimation of the process forces at the honing stone.

There are different ways to estimate the normal force at the honing stone. The direct measurement of the normal force F_n with sensors integrated in the honing tool is described in [3, S. 39]. When large bores are machined (diameter above approximately 50 mm) the tools are large enough to be able to mount the force sensors directly between honing stone and feeding cone.

At small bores (diameter beyond 50 mm) the volume of the sensors in relation to the volume of the tool in the bore is too big to use direct measurement of normal forces at the honing stone. Here, the normal force has to be measured indirectly by calculations from secondary measurements. To calculate the normal force at the honing stone from the axial feeding force the friction at the cone is often neglected. [4, S. 29 f] has intro-

Peer-review under responsibility of the International Scientific Committee of the "15th Conference on Modelling of Machining Operations

doi:10.1016/j.procir.2015.03.066

duced the influence of friction at the cone for a multi stone tool and active feeding movement. [5] states that the torque along the axis of the honing tool is a function of the given constant cutting pressure for each workpiece and therewith a function of the normal force on the honing stone.

To be able to optimize the chip removal process for honing the correlation between the process forces needs to be understood. This paper presents the relations at the tool where the honing stones are in direct contact to the workpiece. The cutting pressure at the honing stone is calculated in different ways and the results are compared.

Nomenclature

γ	cone angle of the honing tool
δ	angle between guiding stones
ϵ	angle between guiding stone 1 and honing stone
μ_h	friction coefficient at the honing stone
μ_{fl}	friction coefficient at the guiding stone
μ_{Steel}	friction coefficient steel-steel
A_k	piston area of the feeding cylinder
b_H	width of one honing stone
c	stiffness of the system of feeding drive, tool and workpiece
d	diameter of the honed bore
$F_{c,t}$	tangential cutting force at the honing stone
$F_{fl,n}$	normal force between guiding stone and workpiece
$F_{fl,t}$	tangential force at the guiding stone
F_n	normal force between honing stone and workpiece
F_k	axial feeding force on the cone
l_B	length of the honed bore
l_H	length of the honing stone
l_h	contact length between honing stone and workpiece
l_{WS}	distance between machine base and lower edge of the honed surface
l_{WZ}	distance between the upper edge of the honing stone and the honing spindle
M_z	torque along the axis of the honing tool
m	number of honing stones
p_k	hydraulic pressure at the feeding cylinder
p_n	cutting pressure at the honing stone
Q_w	material removal rate
$v_{c,a}$	axial component of the cutting velocity
$v_{c,t}$	tangential component of the cutting velocity
$v_{c,r}$	radial component of the cutting velocity
$z(t)$	axial stroke position of the honing spindle

2. Kinematics of the honing process

For long stroke honing of bores, the topic of this paper, the axial cutting velocity $v_{c,a}$ corresponds to the axial stroke movement of the honing tool that oscillates between the upper and lower reversal point. The tangential cutting velocity $v_{c,t}$ results from the rotation of the tool. The radial component of the cutting velocity $v_{c,r}$ is the feeding movement of the honing stone. It is induced by an axial movement of a feeding cone in the honing tool. Figure 1 shows the three movement components and a schematic cut through a honing tool.

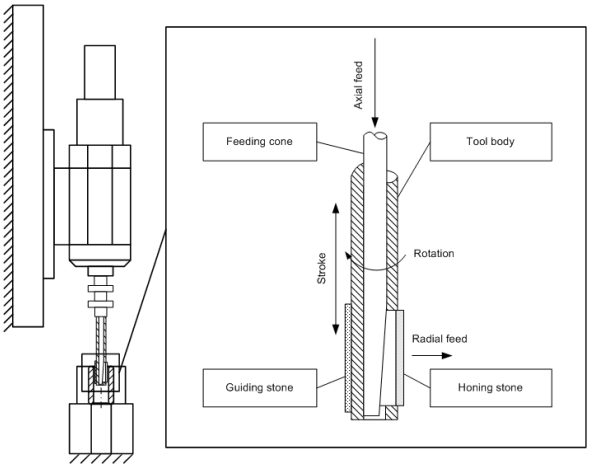

Fig. 1. Movement components of honing and cut through a single stone tool according to [6]

The movement of the feeding cone can be generated either by force-closure or by form-closure principles:

A force-closure principle for moving the feeding cone can be e.g. a hydraulic cylinder. The feeding force depends on the pressure of the hydraulic fluid p_k and the piston area of the feeding cylinder A_k:

$$F_k = f(A_k, p_k) \tag{1}$$

The axial position of the feeding cone is, however, indefinite because there is usually no measuring system for the position of the piston.

For form-closure feeding a mechanical screw gear in combination with a step motor or a servo drive can be used. With the pitch of the thread and the number of steps or the encoder of the servo drive the position of the feeding cone is known very precisely. The feeding force at this principle is, however, indefinite because it depends on the relation between the feeding velocity $v_{c,r}$, the material removal rate Q_w and the stiffness of the system from the feeding drive over the tool to the workpiece c:

$$F_k = f(v_{c,r}, Q_w, c) \tag{2}$$

As an example, Figure 2 shows schematically the paths of the feeding forces for a force-closure and a form-closure feeding principle. The dashed line represents the force from the force-closure system. It changes with a limited velocity, has slurred edges but is approximately constant at the process itself. The continuous line represents the feeding force from the form-closure system. The changing velocities are constant but over the process the force is less constant than the force from the force-closure system. Both paths show a lower level at the end of process. This is called sparking out and used to optimize the surface quality.

3. Modeling

To enable material removal at the honing process the honing stone needs to be moved over the whole surface with a sufficient cutting velocity v_c and a proper cutting pressure p_n [1]. The cutting velocity is assumed to be adequate and not further looked

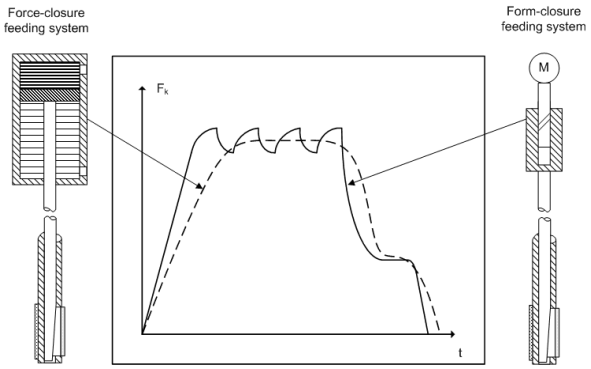

Fig. 2. Paths of feeding forces for a force-closure and a form-closure feeding system according to [7, S. 13]

at in this article. The cutting pressure p_n defines the penetration depth of the cutting grains into the material of the workpiece, the chip formation, the material removal rate and the surface quality of the machined workpiece. It is defined by:

$$p_n = \frac{F_n}{b_H \cdot l_h} \tag{3}$$

The honing stone is pressed against the workpiece with the normal force F_n. The width of the honing stone b_H is given by the geometry of the honing tool and taken as constant. It is assumed that the honed surface does not have any gaps like cross-holes or notches. Thus, the cutting pressure p_n is just dependent on the normal force F_n and the contact length between honing stone and workpiece l_h.

3.1. Contact length

The contact length between honing stone and workpiece $l_h(t)$ is time-dependent as a function of the time-dependent axial stroke position $z(t)$ and the length of the honing stone l_H, the length of the honed bore l_B, the distance between the upper edge of the honing stone and the honing spindle l_{WZ}, and the distance between machine base and lower edge of the honed surface l_{WS}:

$$\begin{aligned} l_h(t) = min(\quad & l_H; \\ & l_B; \\ & l_H + l_{WZ} - z(t) + l_{WS} + l_B; \\ & z(t) - l_{WZ} - l_{WS} \ ) \end{aligned} \tag{4}$$

Figure 3 shows the position of the parameters for the calculation of the contact length.

3.2. Calculation of normal force and cutting pressure

As described in section 1, the direct measurement of the normal force should not be looked at in this paper because for small bores (diameter below 50 mm) there is often not sufficient space in the tool to mount the sensors. Instead the cone force without friction (ideal tool), the cone force with friction (real tool) and the torque along the axis of the honing tool are used.

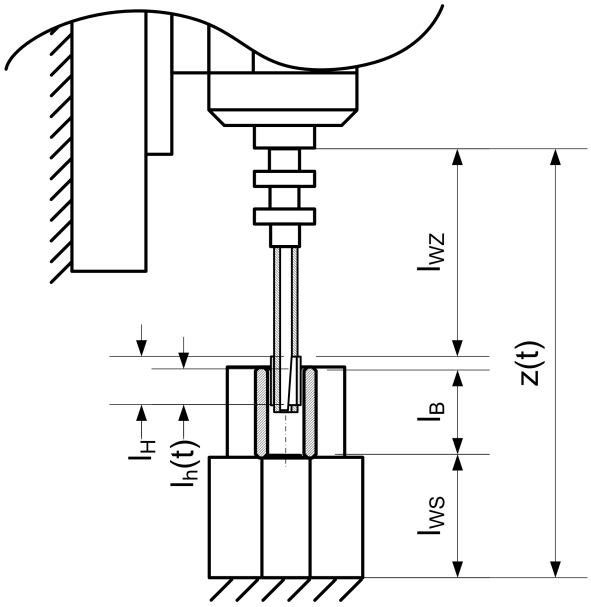

Fig. 3. Parameters for the calculation of the contact length l_h

3.2.1. Normal force calculated from cone force at an ideal tool

With the cone angle γ and the number of honing stones in the tool m, the normal force F_n between honing stone and workpiece can be calculated from the cone force F_k under negligence of frictional forces as:

$$F_n = \frac{F_k}{m \cdot \tan\gamma} \tag{5}$$

With Equation 3, the cutting pressure from the cone force under negligence of friction follows as:

$$p_n = \frac{1}{m \cdot b_H \cdot \tan\gamma} \cdot \frac{F_k}{l_h(t)} \tag{6}$$

3.2.2. Normal force calculated from cone force at a real tool

With inclusion of the frictional forces at the honing tool two cases for the relation between F_n and F_k have to be distinguished. In the first case the normal force F_n at the honing stone is caused by an active downwards movement of the feeding cone by the cone force F_k. [4, S. 29] gives for a multi stone tool ($m > 1$):

$$F_n = \frac{\cos\gamma - 2\mu_{Steel}\sin\gamma}{m\,(\sin\gamma + \mu_{Steel}\cos\gamma)} \cdot F_k \tag{7}$$

With Equation 3, the cutting pressure follows as:

$$p_n = \frac{\cos\gamma - 2\mu_{Steel}\sin\gamma}{m \cdot b_H \cdot (\sin\gamma + \mu_{Steel}\cos\gamma)} \cdot \left.\frac{F_k}{l_h(t)}\right|_{m>1,act} \tag{8}$$

In the second case the direction of the movement is inverted so that the cone is moved upwards by the normal force at the honing stone. This reactive movement may happen by a diminution of the cone force in the process or when the tool goes from a wide to a narrow point in the workpiece. Here,

[4, S. 29] gives the formula for multi stone tools ($m > 1$) as follows:

$$F_n = \frac{\cos\gamma + 2\mu_{Steel}\sin\gamma}{m\,(\sin\gamma - \mu_{Steel}\cos\gamma)} \cdot F_k \quad (9)$$

Again with Equation 3, the cutting pressure follows as:

$$p_n = \frac{\cos\gamma + 2\mu_{Steel}\sin\gamma}{m \cdot b_H \cdot (\sin\gamma - \mu_{Steel}\cos\gamma)} \cdot \left.\frac{F_k}{l_h(t)}\right|_{m>1,react} \quad (10)$$

At single stone tools ($m = 1$) the backside of the feeding cone is not guided by other honing stones, but by the tool body. There, the friction plane is not tilted with the cone angle as at multi stone tools so that the normal force for active feed movement is:

$$F_n = \frac{\cos\gamma - 2\mu_{Steel}\sin\gamma}{\sin\gamma + 2\mu_{Steel}\cos\gamma} \cdot F_k \quad (11)$$

With Equation 3, the cutting pressure can be calculated as:

$$p_n = \frac{\cos\gamma - 2\mu_{Steel}\sin\gamma}{b_H \cdot (\sin\gamma + 2\mu_{Steel}\cos\gamma)} \cdot \left.\frac{F_k}{l_h(t)}\right|_{m=1,act} \quad (12)$$

For single stone tools and reactive feed, i.e. upwards movement of the cone because of high normal force, it follows as:

$$F_n = \frac{\cos\gamma + 2\mu_{Steel}\sin\gamma}{\sin\gamma - 2\mu_{Steel}\cos\gamma} \cdot F_k \quad (13)$$

The cutting pressure follows with Equation 3 as:

$$p_n = \frac{\cos\gamma + 2\mu_{Steel}\sin\gamma}{b_H \cdot (\sin\gamma - 2\mu_{Steel}\cos\gamma)} \cdot \left.\frac{F_k}{l_h(t)}\right|_{m=1,react} \quad (14)$$

3.2.3. Normal force calculated from torque

It is assumed that the chip formation can be handled as a kind of friction within the formula. This has already been stated by [8, S. 236] and [1]. At the honing stone, the tangential cutting force $F_{c,t}$ is proportional to the normal force F_n:

$$F_{c,t} = \mu_h F_n \quad (15)$$

Figure 4 shows a honing tool with $m = 4$ honing stones as an example for the calculation of the forces at a multi stone tool. The forces are indexed counterclockwise from 1 to m. It is assumed that the forces are evenly distributed over the m honing stones.

The equilibrium of the clockwise and counterclockwise torques gives for a tool with m honing stones:

$$M_z = \frac{d}{2} \cdot (F_{c,t1} + F_{c,t2} + \ldots + F_{c,tm}) \quad (16)$$

With (15), it follows as:

$$M_z = \frac{d}{2} \cdot (\mu_h F_{n1} + \mu_h F_{n2} + \ldots + \mu_h F_{nm}) \quad (17)$$

With the assumption mentioned above that the normal forces are equal for all honing stones ($F_{n1} = F_{n2} = \ldots = F_{nm} = F_n$), it follows as:

$$M_z = \frac{m \cdot d \cdot \mu_h}{2} \cdot F_n \quad (18)$$

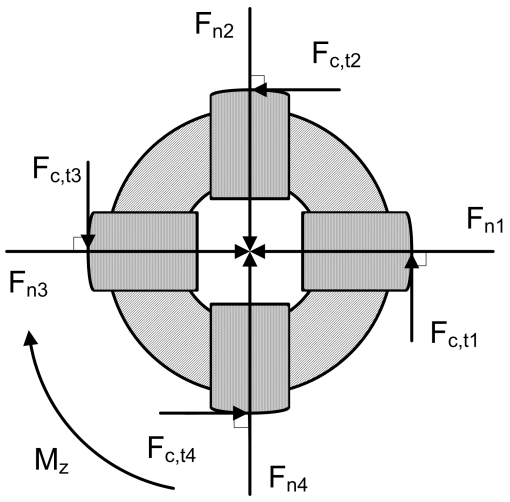

Fig. 4. Directions of forces and torque at a multi stone tool

Solved after the normal force F_n it follows as:

$$F_n = \frac{2}{m \cdot d \cdot \mu_h} \cdot M_z \quad (19)$$

With Equation 3, the cutting pressure can be calculated for the multi stone tool as:

$$p_n = \frac{2}{m \cdot d \cdot b_H \cdot \mu_h} \cdot \left.\frac{M_z}{l_h(t)}\right|_{m>1} \quad (20)$$

For single stone honing tools, the tangential forces at the guiding stones are, similar to (15), also assumed to be proportional to the normal forces:

$$\begin{aligned} F_{fl1,t} &= \mu_{fl1} F_{fl1,n} \\ F_{fl2,t} &= \mu_{fl2} F_{fl2,n} \end{aligned} \quad (21)$$

Figure 5 shows the directions of the normal forces F_n, $F_{fl1,n}$ and $F_{fl2,n}$, of the tangential forces $F_{c,t}$, $F_{fl1,t}$ and $F_{fl2,t}$, the torque along the tool axis M_z and the angles between the guiding stones δ as well as between first guiding stone and honing stone ϵ for a single stone tool.

The equilibrium of the clockwise and counterclockwise torques gives:

$$M_z = \frac{d}{2} \cdot \left(F_{c,t} + F_{fl1,t} + F_{fl2,t}\right) \quad (22)$$

With (15) and (21), it follows as:

$$M_z = \frac{d}{2} \cdot \left(\mu_h F_n + \mu_{fl1} F_{fl1,n} + \mu_{fl2} F_{fl2,n}\right) \quad (23)$$

Over the equilibria of forces in horizontal and vertical direction of Figure 5 and with the assumption that both guiding stones have the same friction coefficient $\mu_{fl1} = \mu_{fl2} = \mu_{fl}$ the forces at the guiding stones can be substituted:

$$M_z = \frac{d}{2} \cdot \left(\mu_h + \mu_{fl} \cdot \frac{-\sin(\delta + \epsilon) + \sin(\epsilon)}{-\sin(\delta)}\right) \cdot F_n \quad (24)$$

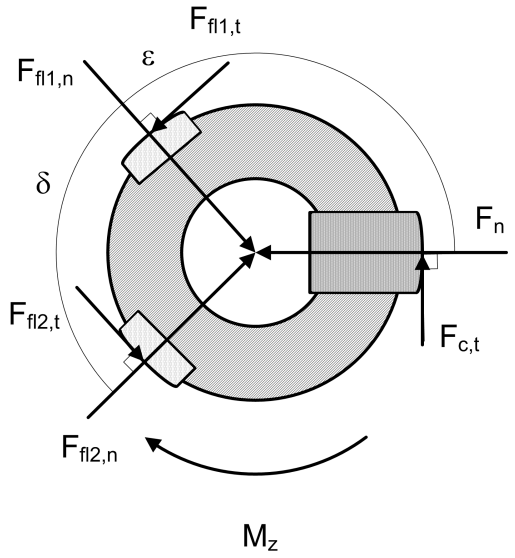

Fig. 5. Directions of forces and torque at a single stone tool

Solved after the normal force F_n it follows as:

$$F_n = \frac{2}{d \cdot \left(\mu_h + \mu_{fl} \cdot \frac{-\sin(\delta+\epsilon)+\sin(\epsilon)}{-\sin(\delta)}\right)} \cdot M_z \tag{25}$$

With Equation 3, the cutting pressure can be calculated for a single stone tool as:

$$p_n = \frac{2}{d \cdot b_H \cdot \left(\mu_h + \mu_{fl} \cdot \frac{-\sin(\delta+\epsilon)+\sin(\epsilon)}{-\sin(\delta)}\right)} \cdot \left.\frac{M_z}{l_h(t)}\right|_{m=1} \tag{26}$$

4. Exemplary paths of cutting pressure

With the parameter set given in Table 1, the paths for the contact length $l_h(t)$ and the cutting pressure p_n are calculated. The course of the contact length is calculated with Equation 4 and given in Figure 6.

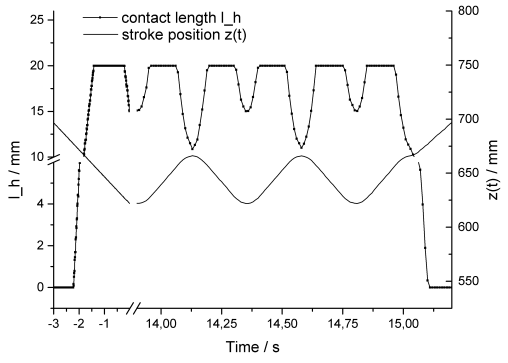

Fig. 6. Contact length calculated from the stroke position

Table 1. Parameters for the example.

Symbol	Parameter	Value	Unit
γ	cone angle of the honing tool	2.5	°
δ	angle between guiding stones	90	°
γ	angle between guiding stone 1 and honing stone	125	°
μ_h	friction coefficient at the honing stone	0.2	
μ_{fl}	friction coefficient at the guiding stone	0.2	
μ_{steel}	friction coefficient steel-steel	0.1	
b_H	width of the honing stone	3	mm
d	diameter of the honed bore	8.0	mm
F_k	axial feeding force on the cone	40	N
l_B	length of the honed bore	50	mm
l_H	length of the honing stone	20	mm
l_{WS}	distance between base and workpiece	309	mm
l_{WZ}	distance between honing stone and spindle	298	mm
M_z	torque along the tool axis	300	N mm
m	number of honing stones	1	
$z(t)$	axial stroke position	622 - 666	mm

The time axis is interrupted from 0 to 13.9 s so that just two complete oscillations of the stroke position $z(t)$ are visible. Before the tool has reached the bore the contact length is zero. When the tool goes into the bore the contact length rises up to 20 mm. When the honing stone leaves the bore at the lower reversal point the contact length decreases to approximately 15 mm. At the upper reversal point the overrun is larger so that the contact length decreases here to approximately 11 mm. This unequal overrun can be used to compensate taper errors at the workpiece.

The calculation of the cutting pressure p_n with Equation 12 and the parameter set from Table 1 is shown in Figure 7.

It is assumed that the force on the cone has been held constant to $p_n = 40$ N. When the contact length is $l_h(t) = 20$ mm the cutting pressure is about $p_n = 2.6 \frac{\text{N}}{\text{mm}^2}$. When the contact length decreases the cutting pressure rises to $p_n = 3.5 \frac{\text{N}}{\text{mm}^2}$ at the lower and to $p_n = 4.5 \frac{\text{N}}{\text{mm}^2}$ at the upper reversal point.

The cutting pressure calculated with Equation 14 and the parameter set from Table 1 is given in Figure 8.

In contrast to Figures 7 and 9, the interrupt of the ordinate is larger to make also visible the range below zero. In this figure the theoretic cutting pressure is negative over the whole range. This implausible result means that the cutting pressure is not able to rise the cone force by a rise of cutting pressure because of friction at the configuration given in Table 1.

Finally, with the assumption of $M_z = 300$ N mm and Equation 26 the cutting pressure has been calculated from the torque. Figure 9 shows the result for the parameter set from Table 1.

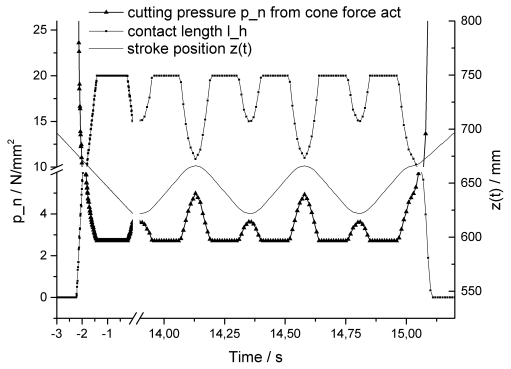

Fig. 7. Cutting pressure from the cone force for active feed, contact length and stroke position

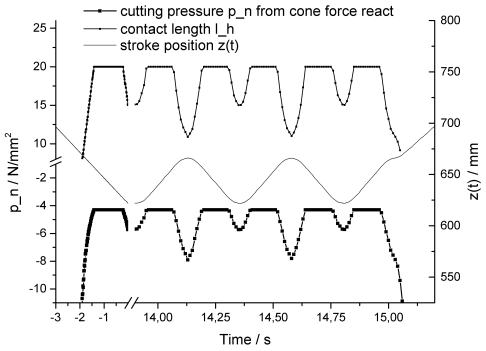

Fig. 8. Cutting pressure from the cone force for reactive feed, contact length and stroke position

The path of p_n corresponds to Figure 7. The values are also approximately equal.

This calculation of cutting pressure from torque M_z has the advantage that the calculated value of cutting pressure is not dependent on the direction of the feeding movement. In contrast, the calculation from the cone force can lead to different results depending on the direction of the feeding movement in case of self-locking at the tool because of large friction as shown in Figures 7 and 8.

5. Conclusion and Outlook

A model of the honing tool and different functional dependencies including perturbations have been shown to estimate the cutting pressure at the honing stone from process loads for single- and multi stone tools. It has been shown that for the axial cone force active and reactive feed have to be distinguished when friction in the tool is included. As an additional indicator for the normal force the torque along the tool axis has been introduced.

An example has been given to show the similarity between the calculation from the cone force at active feed and torque,

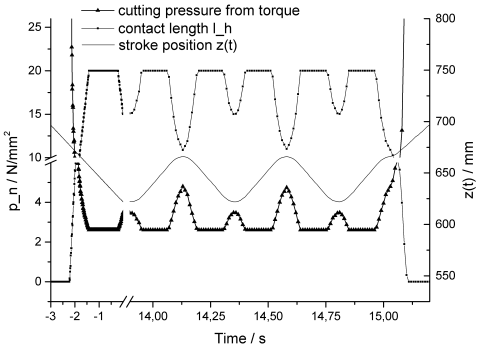

Fig. 9. Cutting pressure from the torque, contact length and stroke position

but also the difference when calculating from the cone force at reactive feed movement in case of self-locking.

This analytical model of a honing tool can now be used to optimize the process control, especially the feeding control, to further enhance the working quality and process capability even for minimal tolerance values.

Acknowledgments

The authors would like to thank the KADIA Production GmbH+Co., Nürtingen, Germany, for the provision of their honing machine and for supporting and funding the investigations.

References

[1] Vrac D, Sidjanin L, Kovac P and Balos S. The influence of honing process parameters on surface quality, productivity, cutting angle and coefficients of friction. Industrial Lubrication and Tribology, Vol. 64 Iss 2 pp. 77 - 83 http://dx.doi.org/10.1108/00368791211208679. 2012.

[2] Schmitt C, Bähre D, Moos U, Forsch K, Klein H, Regler R, Maier R. Kraftregelung zur Erhöhung der Prozessstabilität und Genauigkeit beim Bohrungshonen. Jahrbuch Schleifen, Honen, Läppen und Polieren 66, Vulkan Verlag Essen 2013.

[3] Uebelhör P. Inprocess-Geometriemessung beim Honen. Forschungsberichte aus dem Institut für Werkzeugmaschinen und Betriebstechnik der Universität Karlsruhe, Band 56. ISSN 0724-4967. Karlsruhe, 1994.

[4] Mushardt H. Modellbetrachtungen und Grundlagen zum Innenrundhonen. Berichte aus dem Institut für Werkzeugmaschinen und Fertigungstechnik der TU Braunschweig. VDI Fortschritt-Berichte Reihe 2, Band 117. VDI-Verlag Düsseldorf 1986.

[5] Vrac D, Sidjanin L, Balos S and Kovac P. The influence of tool kinematics on surface texture,productivity, power and torque of normal honing. Industrial Lubrication and Tribology, Vol. 66 Iss 2 pp. 215 - 222 http://dx.doi.org/10.1108/ILT-05-2011-0037. 2014.

[6] Schmitt C, Bähre D, Forsch K, Klein H. Feinstbearbeiten hochgenauer Bohrungen durch Honen. Jahrbuch Schleifen, Honen, Läppen und Polieren 65, Vulkan Verlag Essen 2011.

[7] Plass M. Beitrag zur Optimierung des Honprozesses durch Aufbau einer Honprozeßregelung. Forschungsberichte aus dem Institut für Werkzeugmaschinen und Betriebstechnik der Universität Karlsruhe, Band 91. ISSN 0724-4967. Karlsruhe, 1999.

[8] Saljé E, Von See M. Process-Optimization in Honing. Annals of the CIRP Volume 36 Issue 1 p. 235-239, 1987.